Energy Proceedings
Vol 49, 2024
ISSN 2004-2965

Protection Coordination of Semiconductor Circuit Breakers in Ring-Type 380 V DC Microgrid

Naoki Hanaoka [1], Yuji Higuchi [1], Naruto Arai [1], Kazuya Akiyama [1]

1 NTT Space Environment and Energy Laboratories

(Corresponding Author: naoki.hanaoka@ntt.com)

ABSTRACT

Ring-type DC microgrids (DCMGs) are attracting attention from the viewpoint of expanding the use of renewable energy and improving power resilience. In the short-circuit protection of ring-type DCMG, the direction of current flow is not determined in the ring wiring. Therefore, the method of setting the trip threshold of the circuit breaker that is included in the main line of the ring-type DCMG in steps, as used in the conventional radiation-type DCMG, does not realize protection coordination. Thus, the purpose of this study was to achieve protection coordination of multiple circuit breakers with the same trip threshold in a simpler way. The authors propose a method of enabling protection coordination by combining a semiconductor circuit breaker (SCCB) with a capacitor as an energy source, which is able to interrupt the circuit as soon as the current reaches a threshold. To verify the method, two SCCBs with a trip threshold set at 30 A were connected in series, and four patterns of capacitors (0, 50, 100, and 150 μF) were connected between the SCCBs. The experimental results showed that when the capacitance was 50 μF or less, the current flowing through the SCCB on the power supply side was higher than the trip threshold, and protection coordination could not be achieved in some cases. On the other hand, when the capacitance was 100 μF or more, the current flowing through the SCCB on the power supply side was smaller than the trip threshold, showing that the protection coordination was successful. The experiments demonstrated that short-circuit protection can be coordinated between SCCBs by connecting two SCCBs in series with the same trip threshold and connecting a capacitor of approximately 100 μF or more between the SCCBs.

Keywords: DC microgrid, Protection coordination, Semiconductor circuit breaker, Short-circuit, 3-way SCCB

NONMENCLATURE

Abbreviations	
BESS	Battery energy storage system
DCMG	DC microgrid
MC	Electromagnetic contactor
RE	Renewable energy
SCCB	Semiconductor circuit breaker

1. INTRODUCTION

In recent years, DC microgrids (DCMGs) based on DC power supply have attracted attention from the perspective of expanding the use of renewable energy (RE) and power resilience [1], [2], [3]. DC power supply is more reliable than AC power supply in that it is less prone to power outages and instantaneous voltage drops when combined with a battery energy storage system (BESS) and has therefore been used to supply power to ICT equipment [4], [5], [6]. System architectures and protection technologies similar to DCMGs are also being used in ship internal wiring [7], [8] and wind farms [9]. Thus, the application areas of DCMG-related technologies are expanding, and their importance is growing. Among DCMGs, the ring-type has some advantages over the radiation type, such as a better voltage profile [10]. However, because the ring-type DCMG allows current to flow in both directions, differential trip thresholds cannot be set for the circuit breakers. Therefore, the conventional method of protection coordination in which the trip threshold of each circuit breaker is set in steps cannot be applied to the ring-type DCMG, making protection coordination difficult [11].

Among previously proposed methods for the protection of ring wiring, there is a one that isolates the short-circuit point while estimating the location of the short-circuit point from the transient current that occurs during the short-circuit [12]. However, the previous

This is a paper for the 16th International Conference on Applied Energy (ICAE2024), Sep. 1-5, 2024, Niigata, Japan.

methods have issues, such as increased system complexity and cost.

Therefore, the objective of this paper is to achieve protection coordination of ring wiring in a simpler way. This paper proposes a method to achieve short-circuit protection coordination of ring wiring, which cannot be achieved with conventional circuit breakers, and clarifies the conditions for such coordination.

2. RING-TYPE 380 V DCMG DESCRIPTION

The requirements for the 380 V DCMG assumed in this paper are shown in Table 1. In this system, six sending and receiving points (a total of the main building with BESS and consumers) are connected to a ring wiring via DC/DC converters, as shown in Figure 1. For high reliability, three semiconductor circuit breakers (SCCBs) are installed at each branch point, so that even if a short-circuit accident occurs in the ring wiring, only the SCCB close to the short-circuit point can trip to continue supplying power to all points except the short-circuit point.

The main building equipped with BESS is assumed to be a telecommunication building or data center with backup storage batteries for data communication and connected RE. Due to the cost of installing a BESS, the customer is assumed to have RE but no BESS; the ring wiring must be connected to at least one main building with BESS that will absorb RE fluctuations in the DCMG during normal times and provide commercial power during a disaster. In the event of a commercial power outage during a disaster, the BESS can supply power to any consumer that lacks power, thus ensuring reliability.

The rated voltage between the sending and receiving points is 380 V DC, and the power can be exchanged between the six points. The maximum cable length between the furthest consumers is 4 km and the cable cross-sectional area is 150 mm^2 to keep the voltage drop within 10 %.

In a general radiation-type transmission and distribution network for commercial power consumers, protection coordination can be achieved by setting a larger trip threshold for the circuit breaker on the power plant side and a smaller threshold for the circuit breaker on the consumer side [13]. However, in a ring-type DCMG such as the one shown in Figure 1, the radiation-type method cannot be used because the current direction on the ring wiring is not fixed in one direction. Therefore, a new method is needed in which only the circuit breaker closest to the short-circuit point is tripped

Table 1 Requirements of 380 V DCMG

Item	*Detail*
Main line topology	Ring-type
Maximum cable length	4 km
Cross-sectional area of cable	150 mm^2
Rated voltage	380 V DC
Maximum power of each consumer building	3.8 kW (380 V, 10 A)
Maximum number of buildings	6
Number of the main building with BESS	At least 1

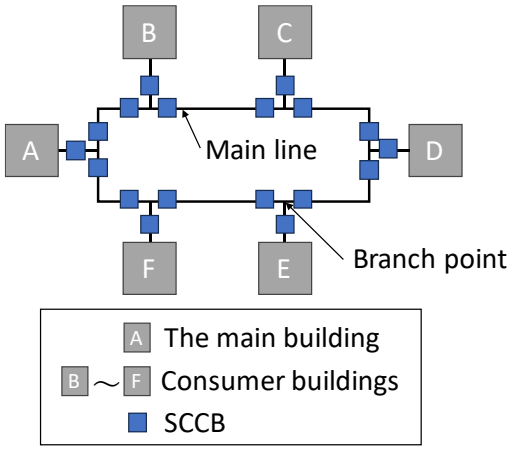

Fig. 1 Ring-type block diagram

while the trip threshold of each circuit breaker is set to the same value.

3. PROPOSAL OF SHORT-CIRCUIT PROTECTION METHOD

The configuration consists of three SCCBs, which are characterized by their ability to trip quickly when the current reaches a threshold value, and a coordination capacitor. The SCCBs are designed to trip only at the short-circuit point by supplying current from the coordination capacitor to the short-circuit point at the time of the short-circuit.

3.1 Semiconductor circuit breaker

To validate the study methodology, an SCCB was developed that meets the requirements to be applicable to the system described in Section 2. The specifications of the developed SCCB are as follows. The rated voltage is 380 V DC, the maximum carrying current is 35 A (continuous), the trip threshold is 30 A, and the break time is within 2 μs. To prevent damage to the SCCB, a varistor (maximum operating voltage of 510 V DC and maximum surge current of 6 kA) is connected to the input and output of the SCCB to suppress the surge

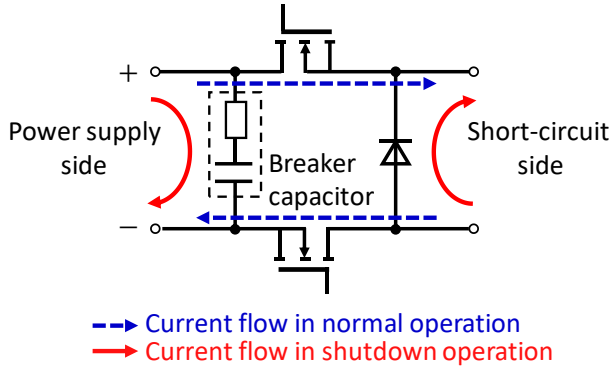

Fig. 2 Circuit configuration for SCCB

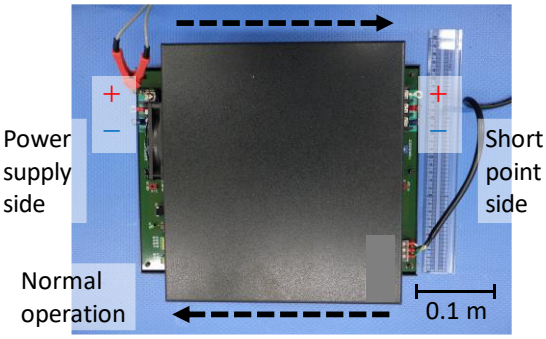

Fig. 3 Prototype of SCCB

voltage below 600 V, the SCCB's breakdown voltage.

Figure 2 shows the main circuit configuration inside the SCCB (blue square) in Figure 1, and Figure 3 shows a photograph of the prototype SCCB. The SCCB can conduct DC current in both directions and has a trip function only for DC current in the normal operating direction as shown in Figure 2 [14]. When the short-circuit current exceeds the 30 A trip threshold, the MOSFETs on the positive and negative lines interrupt the short-circuit current. When the MOSFETs interrupt the circuit, the current path is separated into two circuits (the power supply side and the short-circuit side), and the current flows in the shutdown operation. At this time, the SCCB is subjected to the overvoltage in equation (1), which may damage the SCCB itself or the equipment connected to the ring wiring.

$$V = -L\frac{dI}{dt} \qquad (1)$$

Here, V is the electromotive force [V], L is the inductance [H], and dI/dt is the rate of change of current.

Therefore, a breaker capacitor is connected to the power supply side to charge the current of the power supply current and suppress overvoltage. Also, a freewheeling diode is connected to the short-circuit side to reflux the short-circuit current and suppress overvoltage.

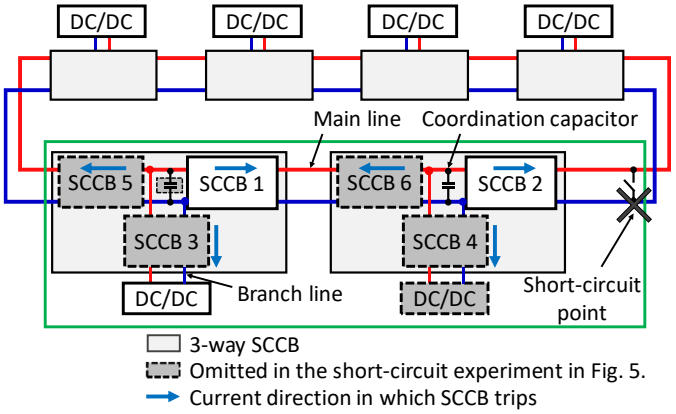

Fig. 4 SCCB position of ring-type block diagram

3.2 3-way semiconductor circuit breaker

The proposed method of coordinating short-circuit protection for ring wiring is to install a 3-way SCCB, which is a combination of three SCCBs and electrolytic capacitors as described in 3.1, at the intersection of the ring wiring and branch lines as shown in Figure 4. Each SCCB is connected at a single point so that the normal direction of operation is outward, and a coordination capacitor is inserted at the connection point. We reasoned that in the event of a short-circuit in the ring wiring, the current from the coordination capacitor would flow preferentially to the short-circuit point, thereby preventing the protective operation of any circuit breaker other than the one immediately adjacent to the short-circuit point. The effect of this capacitor on protection coordination has been studied experimentally.

4. EXPERIMENTAL RESULTS & DISCUSSION

To clarify the coordination conditions for 3-way SCCBs, a verification experiment was conducted using two SCCBs of 3.1.

4.1 Experimental circuit

Experiments were conducted on a simplified system as shown in Figure 5 (the gray area of Figure 4 is excluded) for the case of a short-circuit at the short-circuit point marked with an X in the green area in Figure 4. The simplified system is connected in series as shown in Figure 5 in the order of power supply, SCCB1 on the power supply side, coordination capacitor, SCCB2 on the short-circuit point side, and short-circuit point. The direction of normal operation of SCCB1 and SCCB2 is oriented toward the short-circuit current. The short-circuit point was simulated by an electromagnetic contactor (MC). The cross-sectional area of the electric

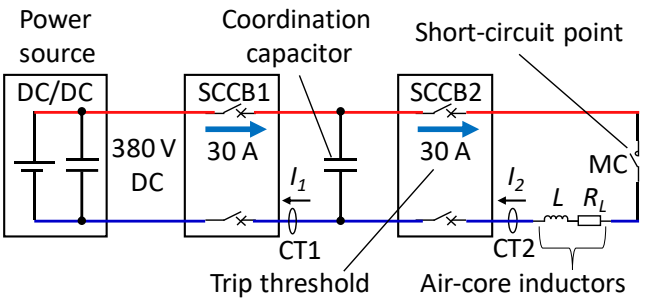

Fig. 5 Experimental circuit

wires connecting the devices is 14 mm^2. The length of the electric wires is about 2.8 m between the power source and SCCB1, about 0.3 m between SCCB1 and the coordination capacitor, about 0.3 m between the coordination capacitor and SCCB2, and about 1.3 m between SCCB2 and the short-circuit point. Since the maximum cable length is 4 km, eight air-core inductors (L: approx. 4 mH, R_L: approx. 3 Ω) simulating a 4 km cable of 150 mm^2 was connected between SCCB2 and MC on the negative line as the main line of the ring wiring. Here, L is the inductance component and R_L is the resistance component of the inductor. In the experiment, a DC voltage of 380 V was applied, and the steady state current was 0 A before the short-circuit occurred.

The reasons for considering that the simplification can be verified are as follows. By excluding the DC/DC converter connected to the branch point immediately above SCCB2 by interrupting it at the nearest SCCB, the current supply to SCCB2 is reduced, and the conditions are such that the circuit breakers are more difficult to coordinate. SCCB3-6 is omitted because it barely affects the direction of the short-circuit current flow. One DC/DC converter is operated in a state where power can be supplied, and the others are omitted because a short-circuit in the ring wiring will cause the circuit to disconnect at the short-circuit point and can be simulated if sufficient current flows from the power supply side of SCCB1 for SCCB1 and SCCB2 to trip. The electrolytic capacitor on the power supply side of SCCB1 is omitted because the X capacitor of the nearby DC/DC converter has a capacitance of about 2000 µF, which is sufficient to trip SCCB1 and SCCB2.

4.2 Effect of coordination capacitor

To verify the coordination conditions of the two SCCBs, the experimental circuit in Figure 5 was used to check how much coordination capacitor would enable coordination when the coordination capacitor was changed. The trip threshold was set to 30 A for both SCCB1 and SCCB2, and the capacitance was set to 0, 50, 100, and 150 µF for the capacitors, considering that they are used in a ring wiring. Whether protection coordination has been achieved is judged by whether the peak value of the current I_1 flowing in SCCB1 exceeds 30 A, which is the trip threshold value.

Figure 6(a) and (b) shows the current waveforms I_1 and I_2 flowing in SCCB1 and SCCB2 during the short-circuit experiment, measured at positions CT1 and CT2 in Figure 5. I_2 remained constant as the coordination capacitor was increased, but the rise of I_1 became slower. This may be because the increase in the discharge current of the coordination capacitor suppressed the increase in the current I_1 flowing from the DC power supply through SCCB1. The reason the I_2 current flows about 25-30 A after the SCCB2 disconnects the circuit is that the current flows through a closed loop between the freewheeling diode inside the SCCB2 and the short-circuit point (MC).

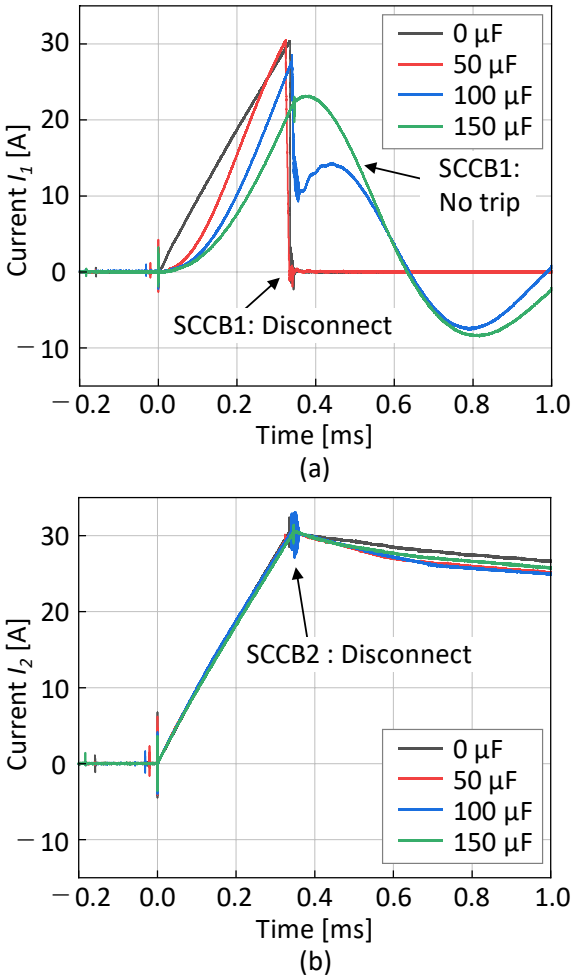

Fig. 6 Current waveform of (a) I_1 and (b) I_2 (capacity comparison)

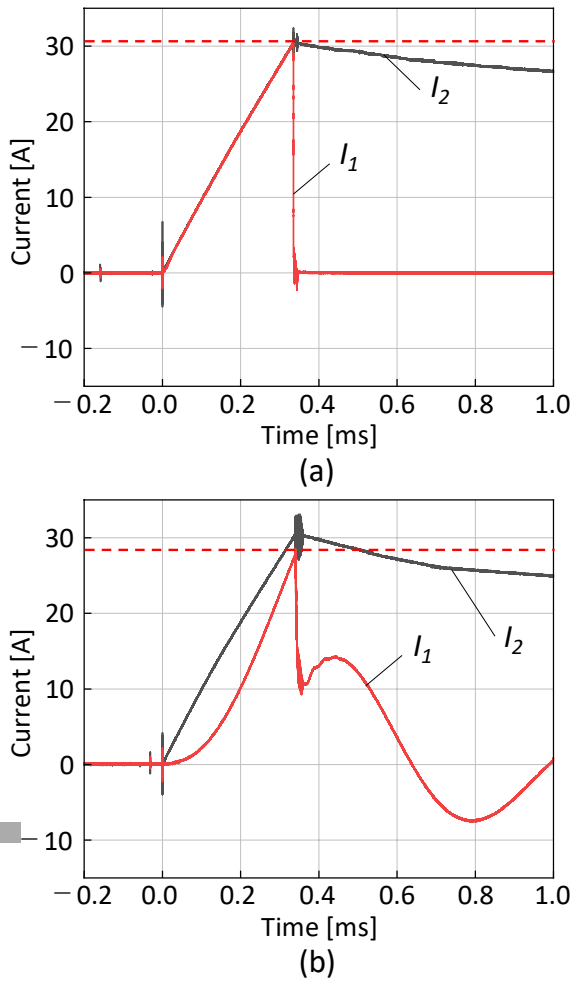

Fig. 7 Current waveform (I_1 vs. I_2) of (a) 0 µF and (b) 100 µF

Figure 7 shows an example of a graph overlaying the current waveforms I_1 and I_2 when determining whether coordination is possible. Figure 7(a) and (b) show the current waveforms when the coordination capacitor is 0, and 100 µF, respectively. The peaks of I_1 (dotted red line) are respectively above and below 30 A in cases (a) and (b), thus showing that the protection coordination fails in case (a) and succeeds in case (b).

Figure 8 shows the maximum value of I_1 when the coordination capacitor is varied. The results of 10 and 3 tests with capacitors of 0 and 50 to 150 µF, respectively, are plotted. When the coordination capacitor was less than 50 µF, the maximum value of I_1 exceeded the SCCB1 trip threshold of 30 A, causing SCCB1 to trip on the power supply side and preventing protection coordination. When the coordination capacitor was 100 µF or more, the maximum value of I_1 could be kept below 30 A, and only SCCB2 could be activated to ensure protection coordination.

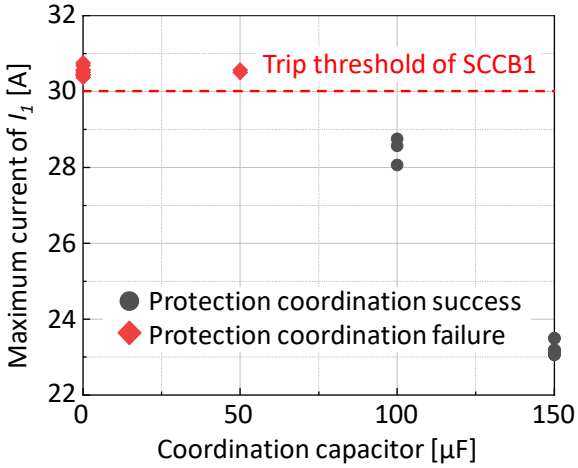

Fig. 8 Coordination capacitor dependence of maximum current of I_1

4.3 Potential implementation issues

The scale of the solution proposed in this paper is a relatively small DCMG with a maximum feeder distance of 4 km and a power of about 3.8 kW for each consumer, as shown in Table 1. On the other hand, from a scalability perspective, considering implementation in larger or more complex DCMG systems reveals the following advantages and potential implementation issues.

- Practicality: Unlike systems that interconnect circuit breakers together for protection [15], our proposed approach allows SCCBs to be installed and operated independently and is likely to remain applicable even as DCMGs become larger and more complex.
- Current limit: Large-scale DCMGs are examples of connecting MW-class generators [16], [17], which require the upper limit of the current rating of the SCCB to be increased to apply our proposed method.
- Voltage limit: Examples of large-scale DCMGs, ranging from tens to hundreds of kilometers in size [18], [19], require voltage to be raised to increase transmission power. To apply the proposed method, the rated voltage of the circuit breaker must be increased.

5. CONCLUSION & FUTURE WORK

This paper proposed a method for high reliability in ring-type 380 V DCMG that enables short-circuit protection to be coordinated at the ring wiring, which cannot be achieved with conventional passive circuit breakers, and experimentally clarified the conditions for such coordination.

When two SCCBs with the same trip threshold are connected in series and the wiring between the SCCB and the short-circuit point is 4 km, we experimentally showed that short-circuit protection coordination between the SCCBs can be achieved by a coordination capacitor of approximately 100 μF or more between the SCCBs.

In the future, we plan to investigate the effectiveness of the proposed short-circuit protection method in detail by conducting experiments and simulation analyses with the line impedance as a variable.

REFERENCE

[1] Bayati, N., Balouji, E., Baghaee, H. R., Hajizadeh, A., Soltani, M., Lin, Z., & Savaghebi, M. (2022). Locating high-impedance faults in DC microgrid clusters using support vector machines. Applied Energy, 308, 118338.

[2] Caparrós Mancera, J. J., Saenz, J. L., López, E., Andújar, J. M., Segura Manzano, F., Vivas, F. J., & Isorna, F. (2022). Experimental analysis of the effects of supercapacitor banks in a renewable DC microgrid. Applied Energy, 308, 118355.

[3] Nishita, Y., Izui, Y., Honda, M., Mizuochi, M., Natsuume, D., & Tabata, H. (2021, 18-21 July 2021). DC Microgrid Experimental System at KIT and its Autonomous Distributed DC Voltage Control Method. 2021 IEEE Fourth International Conference on DC Microgrids (ICDCM).

[4] Babasaki, T., Tanaka, T., Nozaki, Y., Tanaka, T., Aoki, T., & Kurokawa, F. (2009, 18-22 Oct. 2009). Developing of higher voltage direct-current power-feeding prototype system. INTELEC 2009 - 31st International Telecommunications Energy Conference.

[5] Tanaka, T., Hanaoka, N., Takahashi, A., Asakimori, K., Iwato, T., Sakurai, A., & Yamashita, N. (2015, 18-22 Oct. 2015). Concept of new power supply system topology using 380 V and 48 V DC bus for future datacenters and telecommunication buildings. 2015 IEEE International Telecommunications Energy Conference (INTELEC).

[6] Hanaoka, N., Hoshi, H., & Takeda, T. (2019, 17-21 March 2019). Test Circuit Analysis and Evaluation of 400 VDC Appliance Coupler. 2019 IEEE Applied Power Electronics Conference and Exposition (APEC).

[7] Qi, L., Cairoli, P., Pan, Z., Tschida, C., Wang, Z., Ramanan, V. R., Raciti, L., & Antoniazzi, A. (2020). Solid-State Circuit Breaker Protection for DC Shipboard Power Systems: Breaker Design, Protection Scheme, Validation Testing. IEEE Transactions on Industry Applications, 56(2), 952-960.

[8] Cairoli, P., Rodrigues, R., Raheja, U., Zhang, Y., Raciti, L., & Antoniazzi, A. (2020, 23-26 June 2020). High Current Solid-State Circuit Breaker for safe, high efficiency DC systems in marine applications. 2020 IEEE Transportation Electrification Conference & Expo (ITEC).

[9] Fan, X., Shu, J., & Zhang, B. (2018). Coordinated Control of DC Grid and Offshore Wind Farms to Improve Rotor-Angle Stability. IEEE Transactions on Power Systems, 33(4), 4625-4633.

[10] Padayattil, G. M., Thobias, T., Sebastian, J., Thomas, M., & Pathirikkat, G. (2016). Hybrid Ring Microgrid with Coordinated Energy Management Scheme. Procedia Technology, 25, 793-800.

[11] Mohanty, R., & Pradhan, A. K. (2018). Protection of Smart DC Microgrid With Ring Configuration Using Parameter Estimation Approach. IEEE Transactions on Smart Grid, 9(6), 6328-6337.

[12] Mohanty, R., & Pradhan, A. K. (2019). DC Ring Bus Microgrid Protection Using the Oscillation Frequency and Transient Power. IEEE Systems Journal, 13(1), 875-884.

[13] Fani, B., Bisheh, H., & Sadeghkhani, I. (2018). Protection coordination scheme for distribution networks with high penetration of photovoltaic generators. IET Generation, Transmission & Distribution, 12(8), 1802-1814.

[14] Murai, K., Tanaka, T., Babasaki, T., & Nozaki, Y. (2012, 30 Sept.-4 Oct. 2012). Improvement of PDC and PDU with semiconductor breakers. Intelec 2012.

[15] Ko, B. S., Lee, G. Y., Choi, K. Y., Kim, R. Y., Kim, S., Cho, J., & Kim, S. I. (2020). Flexible Control Structure for Enhancement of Scalability in DC Microgrids. IEEE Systems Journal, 14(3), 4591-4601.

[16] Alegria, E., Brown, T., Minear, E., & Lasseter, R. H. (2014). CERTS Microgrid Demonstration With Large-Scale Energy Storage and Renewable Generation. IEEE Transactions on Smart Grid, 5(2), 937-943.

[17] Obara, S. y. (2015). Dynamic-characteristics analysis of an independent microgrid consisting of a SOFC triple combined cycle power generation system and large-scale photovoltaics. Applied Energy, 141, 19-31.

[18] Higashikawa, K., & Kiss, T. (2019). Novel Power System With Superconducting Cable With Energy Storage Function for Large-Scale Introduction of Renewable Energies. IEEE Transactions on Applied Superconductivity, 29(5), 1-4.

[19] Farthing, A., Rosenlieb, E., Steward, D., Reber, T., Njobvu, C., & Moyo, C. (2023). Quantifying agricultural productive use of energy load in Sub-Saharan Africa and its impact on microgrid configurations and costs. Applied Energy, 343, 121131.